Influence of a Coaxial Gas Flow on a Flashing Liquid Jet: Implications for Flame Spray Synthesis of Nanoparticles

H. Vu[1], O. García-Valladares[2], H. Jung[1,3] , and G. Aguilar[1*]
[1]Department of Mechanical Engineering
University of California, Riverside, CA 92521
[2]Centro de Investigación en Energía
de la Universidad Nacional Autónoma de México
Privada Xochicalco S/N, 62580 Temixco, Morelos, México
[3]Center for Environmental Research and Technology
**Riverside, CA 92507**

Abstract

Flashing or thermodynamic breakup of a liquid jet occurs when a pressurized subcooled or saturated liquid is released to a lower pressure, resulting in violent vapor nucleation, expansion, and break up of the liquid phase. Flashing is known to produce very fine droplet atomization, often not possible by traditional mechanical means. In this work, flashing atomization is introduced in a spray burner used in flame spray pyrolysis (FSP). Traditional operation of the spray burner requires atomization of a liquid precursor jet by a coaxial gas flow that also functions as the oxidant and fuel. In this way, the atomization quality of the spray is coupled with the combustion characteristics, particularly flame length. This has made control of nanoparticle characteristics difficult as they are heavily dependent on initial droplet size, temperature profile and flame residence time. The flashing mode of atomization may be introduced by pressurizing and heating the precursor liquid. Under appropriate conditions, this allows for independent control of oxidant/fuel gas flow rate without affecting atomization quality.

This study specifically examines the influence of a coaxial He gas flow on a flashing water jet. New external flashing modes were observed that have not yet been identified that explain the multimodal velocity distributions often measured by PDPA systems for flashing sprays. It was found that flashing under low precursor superheat produced better atomized sprays due to the wind shear by the coaxial gas flow. Higher precursor superheat increased its flow rate and thus decreased the momentum flux ratio between the gas and liquid streams. Hence, measured droplet sizes reverted back to flash-only values with increasing superheat. However, gas flow still had the effect of increasing droplet velocities.

Introduction

Flashing occurs when a pressurized supercritical, subcooled or saturated fluid is released to a lower pressure, resulting in expansion, violent vapor nucleation, and break up of the liquid phase due to thermodynamic instability. Flashing of liquid jets has been studied since the early 1960's [1]. Early works were primarily qualitative visualization studies documenting the phenomenology of the flashing process [2-4]. Later, empirical and semi-theoretical correlations were developed to predict spray properties based on initial conditions, though applicable conditions for these relations were limited [5]. Modeling work of jet breakup and droplet dispersion has also been performed for limited situations [6-8]. Recently, due to advances in spray diagnostics, some quantitative spray characteristic measurements have been performed [9-11] though currently a lack of comprehensive measurements exists and more are needed to facilitate modeling. Interest in flashing continues due to applications in accidental releases of pressurized liquids [12], fuel injection [13], emulsifications [14], and spray cooling [15, 16]. With flashing, fine droplet atomization and narrow size distribution are possible.

Flashing may also be applied to flame spray pyrolysis (FSP) of ceria particles for catalysis of soot from diesel engines [17]. Traditional operation of the spray burner requires atomization of a liquid precursor jet by a coaxial gas flow that also functions as the oxidant and fuel. In this way, the atomization quality of the spray is coupled with the combustion characteristics, particularly flame length. This has made control of nanoparticle characteristics difficult as
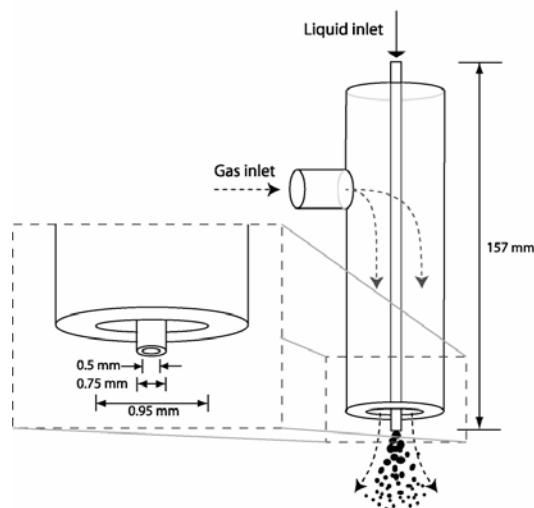
Figure 1. Spray burner geometry.

| PDPA hardware characteristics	
signal processor	FSA 3500
photo detector	PDM 1000
laser	Argon ion
Bragg cell frequency	40 MHz
wavelength	514.5, 488 nm
focal length of transmitting probe	250 mm
focal length of receiving probe	300 mm
laser power	150 mW
slit aperture	25 um
off-axis angle	30 degrees
diameter range	0.59-212.28 um
velocity range	0-235.53 m/s
beam waist	95.13 um
Run settings	
PMT	450 V
signal to noise ratio	med
coincidence mode	coincident
burst threshold	30 mV
band pass filter	5-40 MHz
down mix frequency	35 MHz
refractive index of particle	1.33
Intensity validation	
number of diameter bins	250
slope upper intensity curve	0.180 mV/um/um
lower to upper intensity curve ratio	0.1
upper intensity curve intercept	50.00 mV
lower intensity curve intercept	0.00 mV

Table 1. PDPA Settings

T_{st} [°C]	mass flow rate [kg/h]	void fraction	liquid velocity [m/s]	gas velocity [m/s]
120	0.7672	0.88	9.12	78.60
130	0.8759	0.89	10.89	133.10
140	1.031	0.89	13.10	207.55
150	1.3027	0.90	16.72	302.04
160	1.6209	0.89	20.67	308.87
170	1.9825	0.89	25.01	302.57
180	2.3982	0.89	29.96	307.84

Table 2. Precursor mass flow rate and tube exit flow parameters computed by numerical simulation.

they are heavily dependent on both initial droplet size and flame residence time. Existing research of FSP by others is largely empirical and focused on precursor and fuel choices, flame characteristics and other combustion aspects [18].

The flashing mode of atomization may be introduced to the existing coaxial air-blast atomizer by pressurizing and heating the precursor liquid prior to
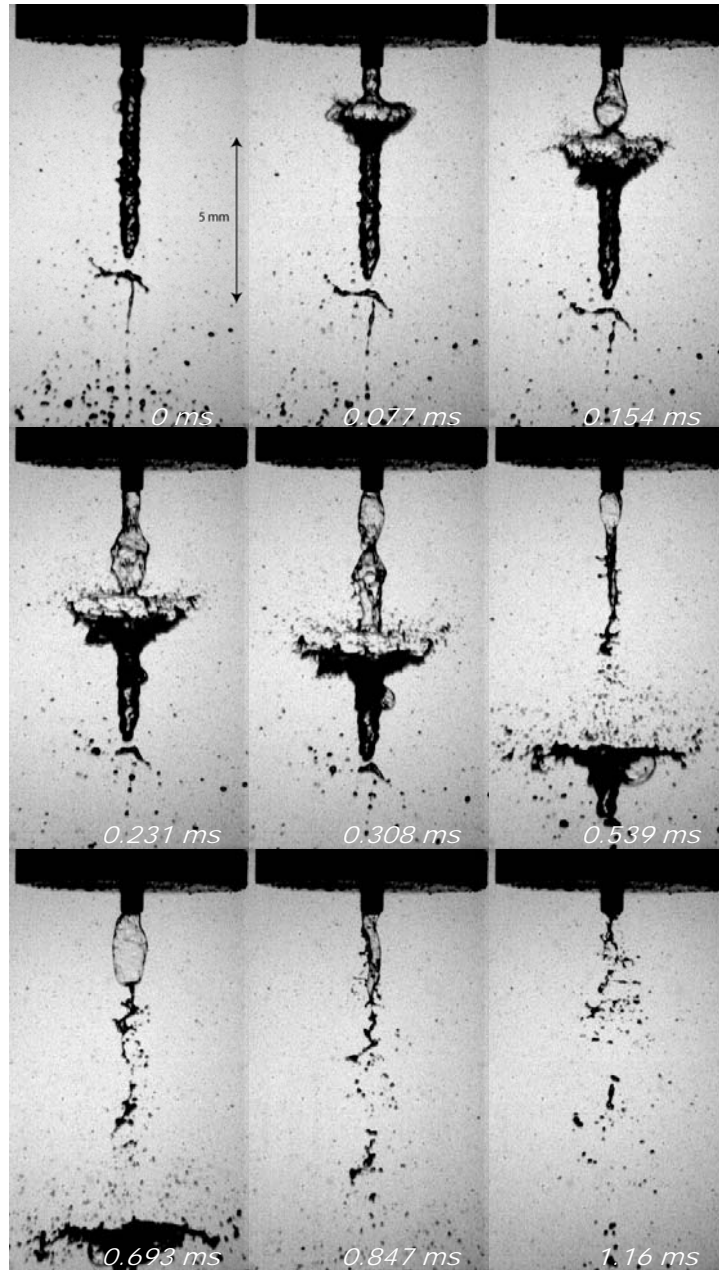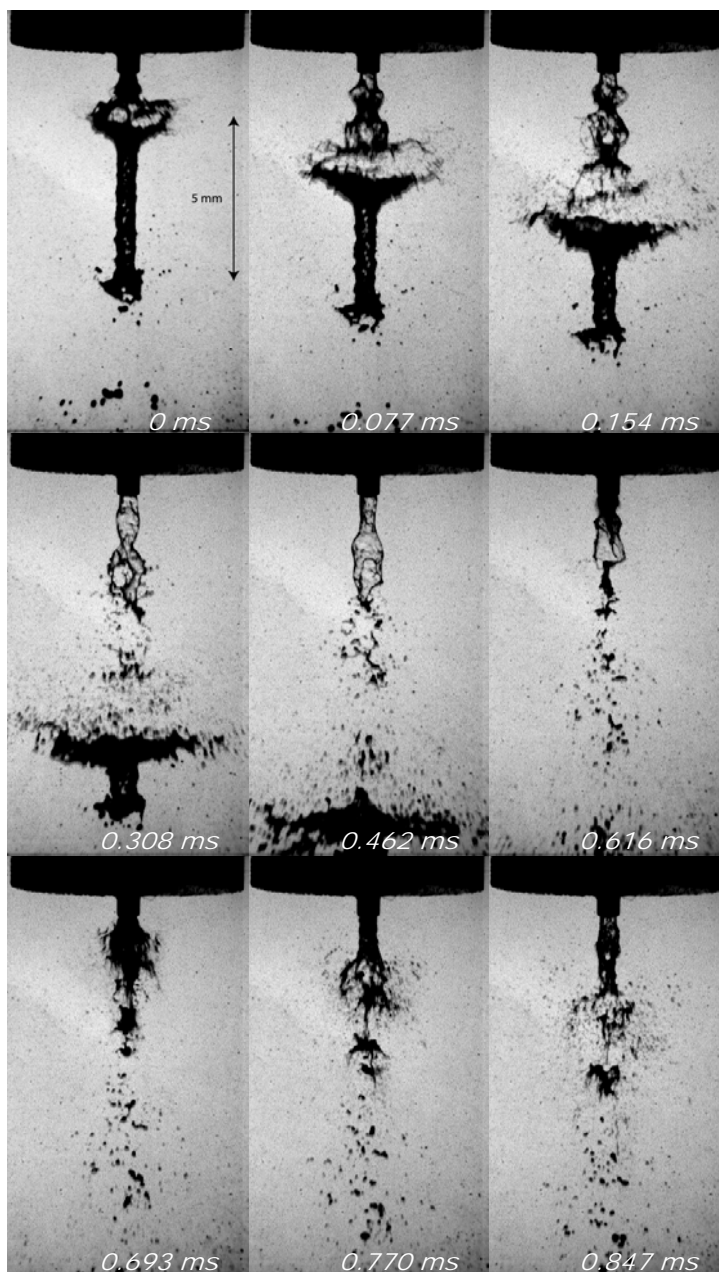
Figure 2. Flashing jet break up of water initially at 120 °C showing a main explosion followed by a wavy wake disintegration of the succeeding jet

injection. Under appropriate conditions, this may allow for independent control of oxidant/fuel gas flow rate without affecting atomization quality. The effects of the coaxial gas flow and presence of the flame are, however, unknown and must be determined.

Desirable droplet characteristics for ceria formation are very small droplet diameters within a narrow,

symmetric distribution to enable more complete combustion of the precursor and more uniform particle sizes. Existing air-blast atomizers will produce droplets in the 10 micron range with a high throughput. An alternative technique using electrosprays will produce more desirable nano-sized droplets, but have much lower throughput [19]. The incorporation of flashing phenomena to the air-blast atomizer may
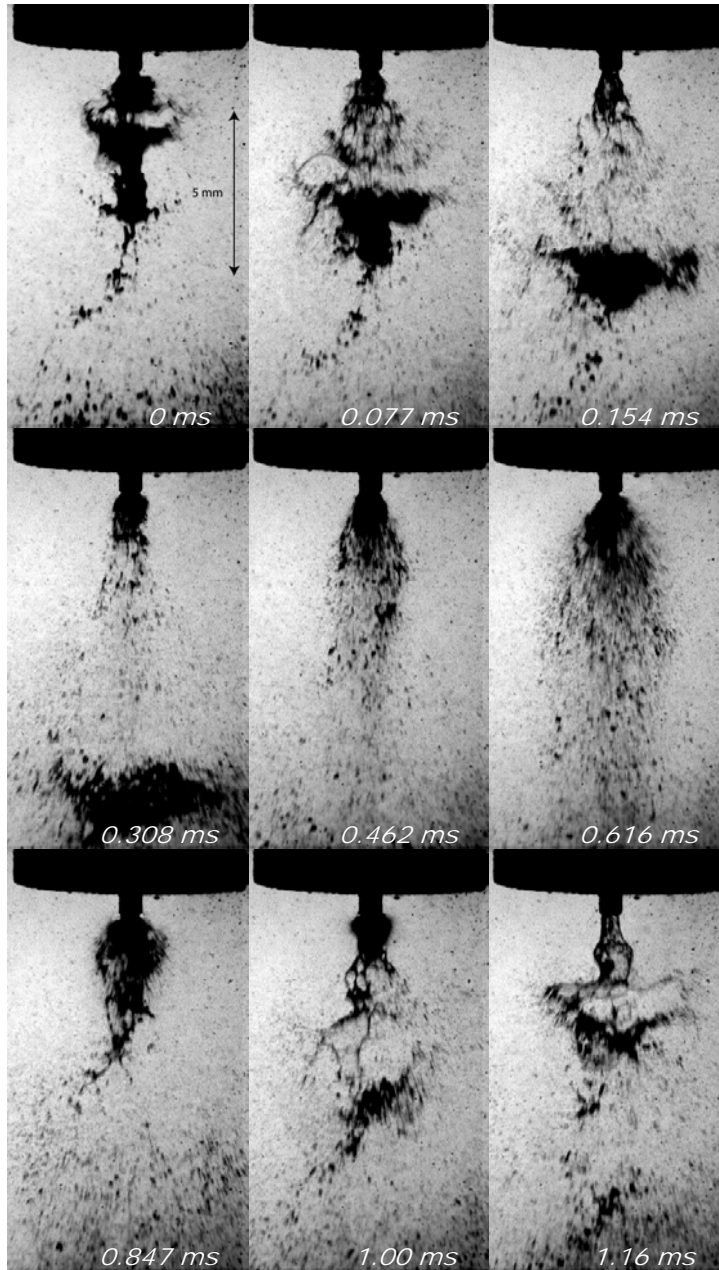
Figure 3. Flashing jet break up of water initially at 140 °C showing a main explosion followed by a partial wavy wake disintegration of the succeeding jet and secondary explosion.

improve control of atomization and reduce droplet sizes while still maintaining high throughput, allowing for future scale-up of particle production.

Materials and Methods

As depicted in Figure 1, a coaxial spray burner currently used in nanoparticle production is also used for this study. For safety reasons, water and helium are used as substitutes for the methanol precursor and hydrogen co-flow. Prior to its delivery to the spray burner, water is kept at saturation in a sealed, stainless steel storage cylinder and heated to initial storage temperatures (T_{st}) of 120-180 °C in 10°C increments using a band heater. A type-K thermocouple, placed inside the cylinder, is attached to a feedback controller used to control the band heater power. Because this is a preliminary study, He co-flow is kept fixed at a flow rate of either 0 or 15 ml/min us-
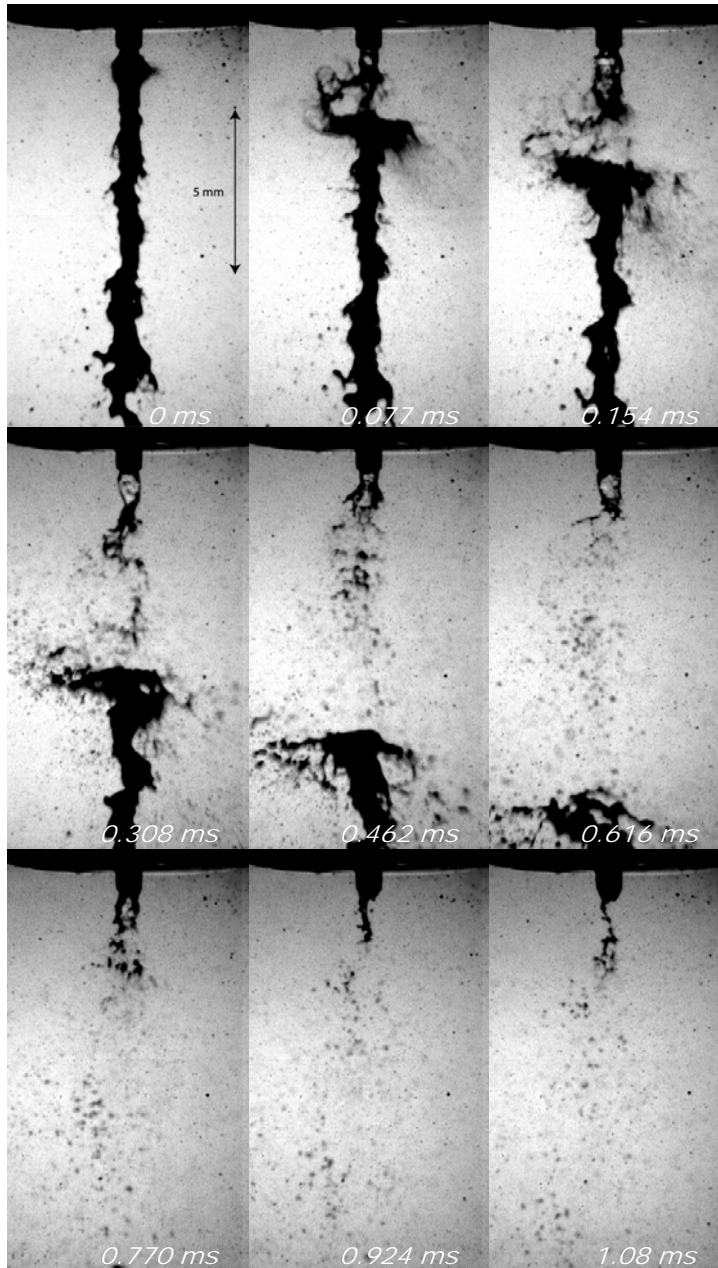
Figure 4. Flashing jet break up of water initially at 150 °C showing intermittent external explosions with flare flashing.

ing a gas flow controller to observe the effects of a coaxial flow.

Because of the difficulty in measuring the total water flow rates for each given initial temperature, they are computed using an existing two-phase semi-empirical numerical model [20-22]. The one-dimensional model assumes separated flow, in which the liquid and gas velocities are treated independently. The model computes the internal flow proper-ties along the inner tube of the spray burner by itera-tively varying flow rate to satisfy the mass, momen-tum, energy, and entropy conservation equations. The model requires knowledge of void fraction and fric-tion factor, determined from correlations by Rouhani and Axelsson [23], and Churchill [24] and Friedel [25], respectively. For the current study, the model is used to compute the total flow rate of water, and the liquid and gas phase velocities at the exit of the inner

Figure 5. Flashing jet break up of water initially at 120 °C showing a main explosion followed by a wavy wake disintegration of the succeeding jet

tube. This model has been validated and used by our group previously [26] and has been described in several publications noted above. The reader is referred to these for further details.

To characterize the external break up properties of the emerging jet, both high-speed video imaging and PDPA measurements are used. We use a high-speed Phantom camera (Vision Research Inc., Wayne, NJ) set at 13000 fps along with a Nikkor lens with +6 magnification lenses. The imaged area is backlit by a halogen lamp with diffuser. The PDPA system (TSI Inc., Shoreview, MN) is set to measure at the center of the external flow, 15 mm from the spray burner tip. A minimum of 10000 validated signals are taken for each initial water temperature. PDPA settings are given in Table 1.
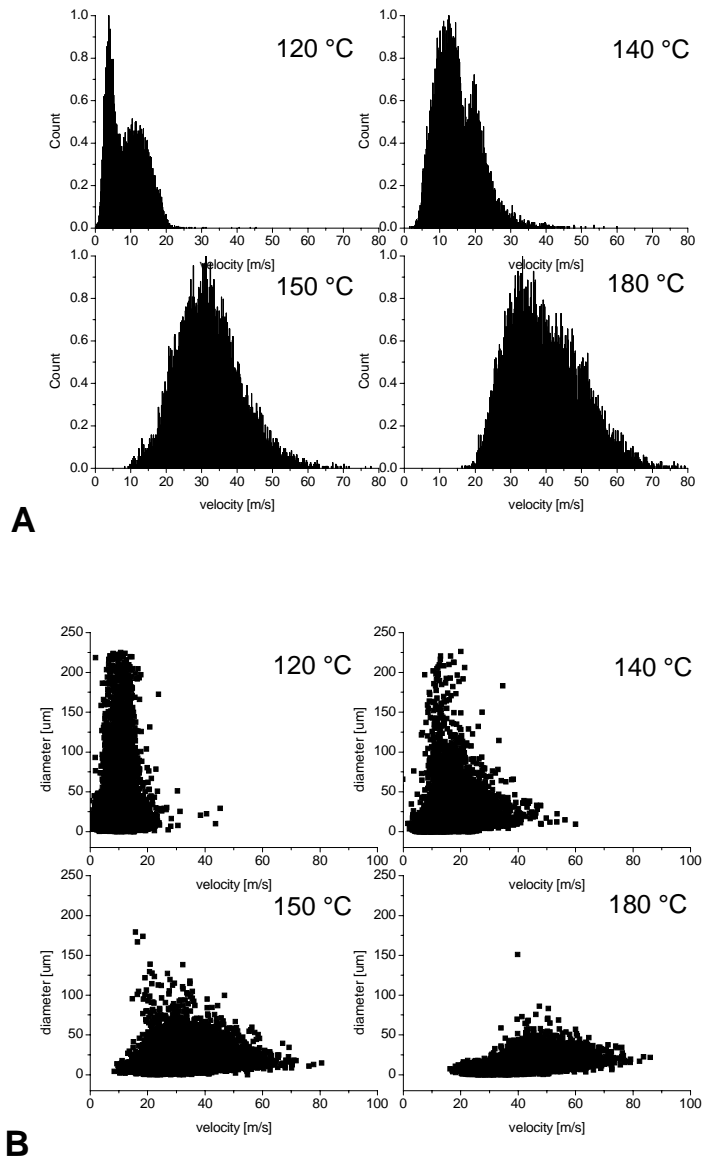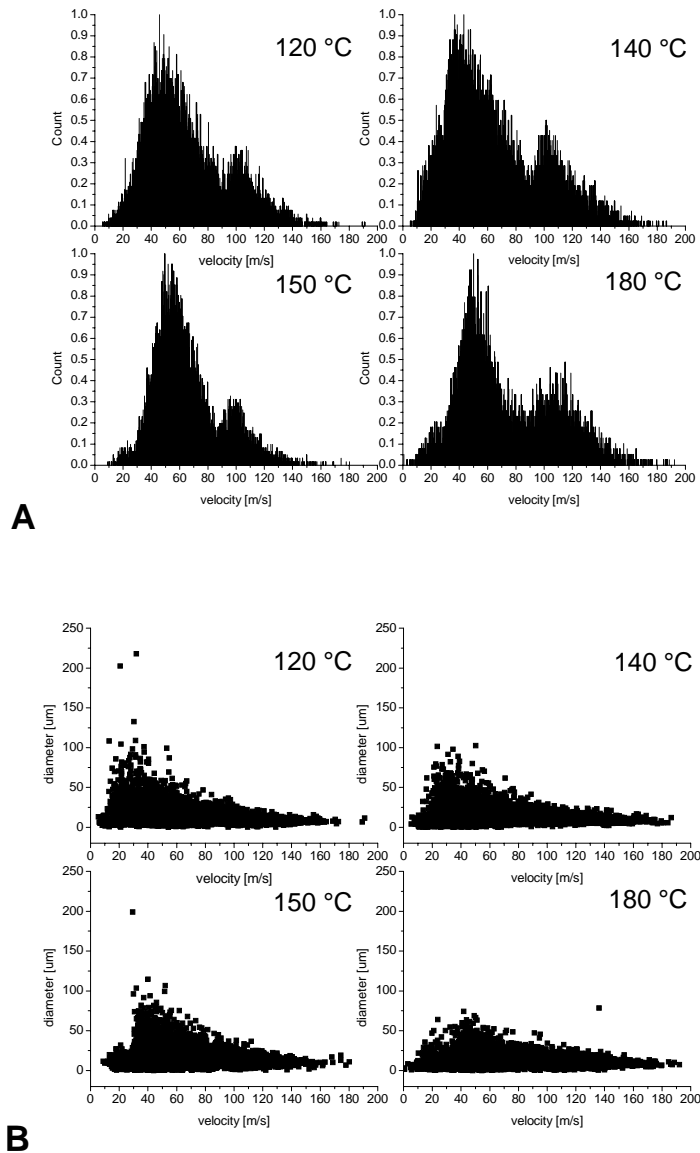
Figure 6. PDPA measured (**A**) velocity histograms and (**B**) diameter vs. velocity distributions without coaxial gas flow.

Results and Discussion

Table 2 provides the mass flow rates of water as well as exit void fraction and phase velocities computed by the numerical model. It is clear that increasing the initial storage temperature of the water can increase its flow rate significantly for a fixed nozzle geometry. This is an important consideration when weighing atomization quality versus FSP production rate.

The high-speed video imaging reveals different modes of jet break up not previously observed in flashing studies. Figure 2 depicts a breakup sequence for water initially at 120 °C. Initially, the water emerges as an unbroken jet. Occasionally, however, a nucleated bubble within the jet will burst at some point downstream of the tube exit. This causes the liquid to explode and disintegrate radially, while the jet below the expansion remains an intact slug. Occasionally, other bubbles appear to nucleate and expand within this slug, though further bulk disintegration by

Figure 7. PDPA measured (**A**) velocity histograms and (**B**) diameter vs. velocity distributions with coaxial gas flow.
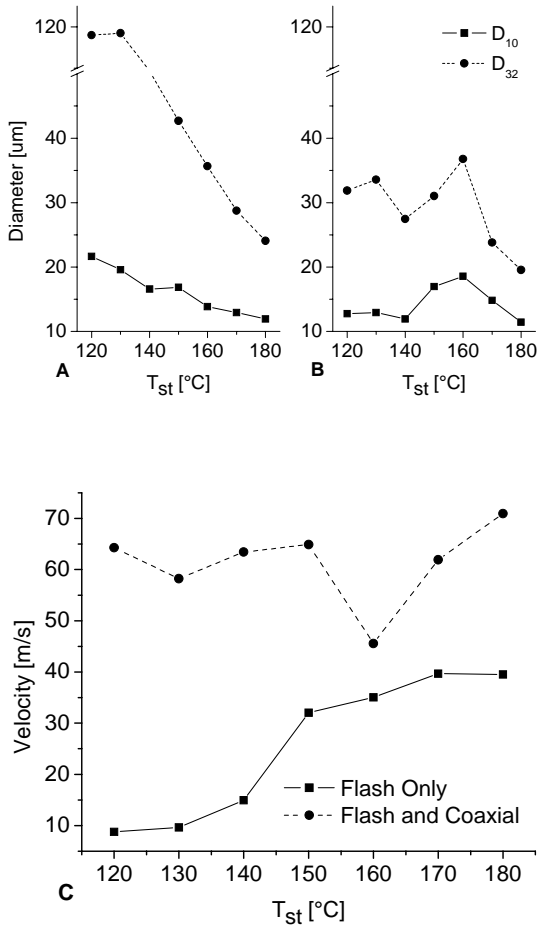
expansion is not observed within the field of view. Further breakup of the slug likely occurs by aerodynamic forces further downstream. Above the point of main explosion, a wake is created which greatly affects the succeeding flow. A wave with characteristic wavelength and amplitude grows and persists for typically two to three cycles. As each cycle collapses, it will disintegrate into droplets with the same axial velocity as the unbroken jet. Unlike droplets formed by the main explosion, they have nearly zero radial velocity. In some instances, following the break up

sequence, an extended period may exist in which only water vapor emerges from the tube.

As the water temperature is increased, the frequency of the break up sequences increases. Several main explosions may occur in succession, preventing the formation of wave break up. At 140 °C (Figure 3), a transition is observed in which the main explosion may be followed by a smaller explosion of lower intensity that occurs within the wake.

Increasing the temperature to 150 °C (Figure 4) results in nearly continuous break up, such that an

Figure 8. PDPA measured (**A**) average diameter without coaxial flow, (**B**) average diameter with coaxial flow, and (**C**) average velocity.

are analogous for higher temperatures. However, after initiation of flare flashing at 150-160 °C, the coaxial flow appears to have little effect aside from acceleration the droplet velocities. These latter scenarios are, again, not shown for brevity.

Quantitative droplet characteristics are provided by PDPA measurements. Velocity histograms and diameter vs. velocity plots are provided in Figures 6 and 7 for flash only and flash and coaxial flow, respectively. A bimodal distribution of velocity is observable in flash only at 120 and 140 °C. This may be attributed to the explosive and wavy modes of break up observed in the imaging. The higher velocity mode may represent the explosive break up due to the acceleration from explosion. As temperatures increase and the flow transitions to more uniform breakup characteristics, the bimodality disappears. Diameter distributions show that droplet sizes decrease significantly with increasing temperature. Droplets also shift to higher velocities and the overall velocity distribution widens. With the coaxial He flow, the velocity histograms show bimodality throughout the temperature range of the study. The higher velocity mode may be attributed to acceleration from the coaxial flow. The velocity appears to shift to higher values with increasing temperature, though relative distribution remains fairly constant. Diameter vs. velocity plots also show a wide spread in velocity with little change in distribution.

D_{10} and D_{32} averages and mean velocities are shown in Figure 8. Interestingly, the average droplet sizes achievable at low superheat with coaxial flow are nearly the same as that for high superheat. There is also a trend of increasing droplet size within the
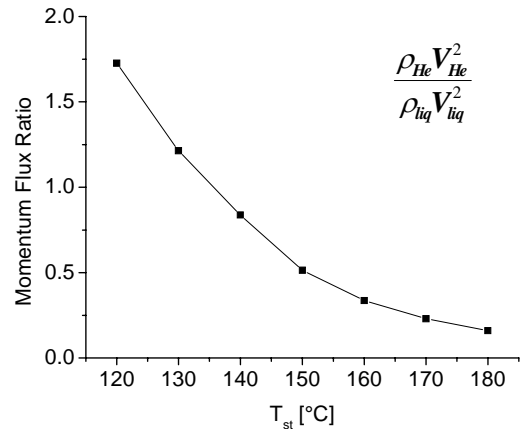
unbroken jet rarely exists. Primary and secondary explosions occur with high frequency and intensity. Additionally, "flare flashing" may occur, as identified by Peter et al, in which a finely atomized spray exits at the tube exit. The unbroken slug identified for 120 °C no longer exits. Increasing the temperatures beyond 150 °C causes the flare flashing break up mode to occur continuously but with pulsating intensity. By 170-180 °C, stable flare flashing is achieved. These latter scenarios are not shown for brevity.

Figure 5 illustrates the effect of the addition of coaxial He gas on a 120 °C water jet. Strong wind shear is evident on the unbroken jet, resulting in some first-wind induced breakup. Primary explosions occur as without the coaxial flow, but with resulting droplets being accelerated by the gas flow. The succeeding wake is now strongly subjected to wind shear and breaks up more finely than before. The effects

Figure 9. Momentum flux ratio of coaxial gas to liquid vs. initial liquid storage temperature.

temperature range of 140-160 °C. Since the coaxial gas flow rate is kept constant as the liquid flow rate increases, atomization by wind shearing becomes less important as superheat increases. Therefore, droplet sizes tend to revert back to those without coaxial flow. This trend may be demonstrated by plotting momentum flux ratio vs. T_{st} as shown in Figure 9.

Conclusions

Flash atomization was introduced into an existing spray burner used for flame spray pyrolysis to observe the atomization phenomena and influence of a coaxial gas flow. Different modes of flashing breakup (*primary* and *secondary explosive* and *wavy*) were identified that have not previously been observed. Through numerical modeling, the mass flow rate was found to increase significantly with increasing initial temperature. The addition of a coaxial flow tends to destabilize the liquid jet by wind shear and accelerate the formed droplets. Droplet sizes decreased significantly with coaxial flow for lower superheats. However, as super heat increased, droplet sizes reverted back to flash-only values due to the decreasing momentum flux ratio between the gas and liquid streams. Bimodal distributions were observed in PDPA measurements and were attributed to multimodal flashing breakup and acceleration due to the coaxial gas flow. Future studies are needed to modify the mass flow rate of the liquid precursor by changing the inner tube diameter and determine if higher momentum flux ratios will further decrease droplet sizes for high superheat cases.

References

1. Brown, R. and York, J.L., *Aiche Journal* 8:149-153 (1962).
2. Peter, E.M., Takimoto, A., and Hayashi, Y., *Jsme International Journal Series B-Fluids and Thermal Engineering* 37:313-321 (1994).
3. Reitz, R.D., *Aerosol Science and Technology* 12:561-569 (1990).
4. Park, B.S. and Lee, S.Y., *Atomization and Sprays* 4:159-179 (1994).
5. Kitamura, Y., Morimitsu, H., and Takahashi, T., *Industrial & Engineering Chemistry Fundamentals* 25:206-211 (1986).
6. Zeng, Y.B. and Lee, C.F.F., *Combustion Science and Technology* 169:45-67 (2001).
7. Sher, E. and Elata, C., *Industrial & Engineering Chemistry Process Design and Development* 16:237-242 (1977).
8. Sher, E. and ZeigersonKatz, M., *Atomization and Sprays* 6:447-459 (1996).
9. Allen, J.T., *Journal of Loss Prevention in the Process Industries* 11:291-297 (1998).
10. Allen, J.T., *Journal of Loss Prevention in the Process Industries* 11:299-306 (1998).
11. Knubben, G. and van der Geld, C.W.M., *Applied Thermal Engineering* 21:787-811 (2001).
12. Bowen, P.J. and Shirvill, L.C., *Journal of Loss Prevention in the Process Industries* 7:233-241 (1994).
13. Senda, J., et al., *Jsme International Journal Series B-Fluids and Thermal Engineering* 37:931-936 (1994).
14. Helfgen, B., Turk, M., and Schaber, K., *Journal of Supercritical Fluids* 26:225-242 (2003).
15. Nelson, J.S., et al., *Archives of Dermatology* 131:695-700 (1995).
16. Hsieh, S.S. and Tsai, H.H., *Archives of Dermatological Research* 298:82-95 (2006).
17. Madler, L., Stark, W.J., and Pratsinis, S.E., *Journal of Materials Research* 17:1356-1362 (2002).
18. Kammler, H.K., Madler, L., and Pratsinis, S.E., *Chemical Engineering & Technology* 24:583-596 (2001).
19. Lenggoro, I.W., et al., *Analytica Chimica Acta* 585:193-201 (2007).
20. Escanes, F., Perez-Segarra, C.D., and Oliva, A., *International Journal of Refrigeration-Revue Internationale Du Froid* 18:113-122 (1995).
21. García-Valladares, O., Perez-Segarra, D.C., and Oliva, A., *Applied Thermal Engineering* 22:173-182 (2002).
22. García-Valladares, O., *Applied Thermal Engineering* 24:949-966 (2004).
23. Rouhani, S.Z. and Axelsson, E., *International Journal of Heat and Mass Transfer* 13:383-393 (1970).
24. Churchill, S.W., *Chemical Engineering* 84:91-92 (1977).
25. Friedel, L., *European Two-Phase Flow Group Meeting*, Ispra, Italy, 1979, pp. Paper E2.
26. Vu, H., García-Valladares, O., and Aguilar, G., *International Journal of Heat and Mass Transfer (in press)*.